# Surface integration of ship-motion Green function

**X.B. Chen**[1], **Y.M. Choi**[2], **M.Q. Nguyen**[1] and **P-Y Wuillaume**[1]

[1]Research Department, Bureau Veritas Marine & Offshore, Paris, France
[2]Dept. Naval Architecture and Ocean Engineering, PNU, Busan, Republic of Korea

xiao-bo.chen@bureauveritas.com

Free-surface potential flow associated with a distribution of singularities on a boundary surface, called *super Green function* by Noblesse *et al.* in [1], is studied here for the special case of two flat panels essential in obtaining the kernel elements constructing the boundary integral equations. Unlike the zero-speed case where the free-surface Green function oscillates at a unique wavenumber associated with one frequency, the ship-motion Green function presents high oscillations associated with several groups of wavenumbers for one encounter frequency, such that the numerical integration of the Green function and its gradient becomes extremely difficult. Analytical formulations are then developed for the accurate integration and presented here.

## 1 Introduction

The fundamental solution to ship-motion problems, known as the ship-motion Green function associated with a pulsating and translating source, has been much studied as collected in [2], and summarized in [3]. There are two parameters including wave encounter frequency and ship forward speed. Except the special case of the zero-speed Green function, the most notable characteristic of Green functions for non-zero speed cases is the presence of peculiar singularities and rapid oscillations as field points approach the track of the source point, when both are near the free surface. This behavior was initially observed by Ursell [4] for the zero-frequency case and later investigated by Chen & Wu [5] in a more general context for any combination of frequency and speed. This peculiar behavior poses challenges when computing waterline integrals in classical Boundary Integral Equation (BIE) formulations. More difficulties arise in computing the free-surface integrals involved in the New BIE [6] including integrals on the free surface, to account for interactions with the base flows. To remove this unphysical feature of the Green function, an introduction of viscous effects based on the linearized Navier-Stokes equations has been formulated and analysed in [3]. The ship-motion Green function with viscous effects presents many sound features useful in numerical schemes.

Still the Green function with viscous effects is not directly useful, as the boundary integral equations involve distributions of singularities (sources or sources plus dipoles). Integrations of point Green function on panels of ship hull and free surface associated with distributions of singularities are to be evaluated in an accurate and efficient way. The representation of Havelock's type is a single integral of Fourier polar angle in which a special function called wavenumber integral function in [3] is involved. The surface integral of Green function becomes the integral of the wavenumber integral function. An appropriate application of the integral theorem of Stokes leads to convert the surface integral to the line integral along the surface contour. The line integral is then formulated as the sum of values of antiderivatives of different order at the nodes. In this way, the surface integration of the integrand function in the Fourier polar integral is analytically obtained. Finally, a numerical scheme based on Gauss quadrature is developed to evaluate the single integral and shown to be accurate and efficient to obtain super Green function.

## 2 Ship-motion Green fucntion

We define a Cartesian coordinate system $(o-xyz)$ moving at the same constant speed $U$ as the ship along the positive $x$ direction, by choosing its $(x,y)$ plane to coincide with the undisturbed free surface and the $z-$axis oriented positively upward. In the moving coordinate system $(o-xyz)$, the source is located at $\boldsymbol{\xi}=(\xi,\eta,\zeta)$ and pulsating at a frequency denoted as $\omega_e$. In this gravity-dominant fluid domain, the reference length $L$, the acceleration of gravity $g$ and the water density $\rho$ are used to define the nondimensional coordinates $\mathbf{x}=(x,y,z)$, the time $t$, the fluid velocity $\mathbf{u}=(u,v,w)$, the velocity potential $\Phi$ and the dynamic pressure $P$ with respect to $(L,\sqrt{g/L},\sqrt{gL},\sqrt{gL^3},\rho gL)$, respectively, while the nondimensional frequency $\omega$, the Froude number $F_{\rm r}$ and the Brard number $\tau$ are scaled by

$$(\omega;F_{\rm r};\tau)=\left(\omega_e\sqrt{L/g};U/\sqrt{gL};U\omega_e/g\right) \tag{1}$$

respectively. The fundamental solution to time-harmonic ship-motion problems is written as

$$\tilde{G}(\mathbf{x},\boldsymbol{\xi},t)=\left\{G(\mathbf{x},\boldsymbol{\xi})\mathrm{e}^{-\mathrm{i}\omega t}\right\}\quad\text{with}\quad 4\pi G(\mathbf{x},\boldsymbol{\xi})=-1/r+1/r'+G^F(\mathbf{x},\boldsymbol{\xi}) \tag{2}$$

in which $r$ is the distance from the field point $\mathbf{x}=(x,y,z)$ to the source point $\boldsymbol{\xi}=(\xi,\eta,\zeta)$ and $r'$ is that to the mirror soure point $\boldsymbol{\xi}'=(\xi,\eta,-\zeta)$. The free-surface term $G^F(\mathbf{x},\boldsymbol{\xi})$ is initially defined by a double Fourier integral (with resepct to wavenumber and polar angle) and given in [3] after integration on wavenumber by

$$G^F(\mathbf{x},\boldsymbol{\xi})=\frac{1}{\pi}\int_{-\pi}^{\pi}F(Z,\theta)\,\mathrm{d}\theta\quad\text{with}\quad F(Z,\theta)=A_1K(Z,k_1)+A_2K(Z,k_2)+A_3K(Z,k_3) \tag{3}$$

in which three complex wavenumbers denoted by $k_{1,2,3}(\theta)=\kappa_{1,2,3}(\theta)+\mathrm{i}\mu_{1,2,3}(\theta)$ are determined by the cubic equation

$$(F_{\mathrm{r}}k\cos\theta-\omega)^2-k-\mathrm{i}4\epsilon F_{\mathrm{r}}^3(F_{\mathrm{r}}k\cos\theta-\omega)k^2=0 \tag{4}$$

with the non-dimensional coefficient $\epsilon=\mu g/(\rho U^3)$ involving $\mu$ the fluid dynamic viscosity. The amplitude coefficients

$$\begin{aligned}
A_1&=A_1(\theta)=\mathrm{i}k_1/[4\epsilon F_{\mathrm{r}}^4\cos\theta(k_1-k_2)(k_1-k_3)]\\
A_2&=A_2(\theta)=\mathrm{i}k_2/[4\epsilon F_{\mathrm{r}}^4\cos\theta(k_2-k_3)(k_2-k_1)]\\
A_3&=A_3(\theta)=\mathrm{i}k_3/[4\epsilon F_{\mathrm{r}}^4\cos\theta(k_3-k_1)(k_3-k_2)]
\end{aligned} \tag{5}$$

are dependent on the wavenumbers. Both $k_{1,2,3}$ and $A_{1,2,3}(\theta)$ are symmetric function of the polar angle. Furthermore, the complex variable $Z$ is defined by

$$Z=Z(\mathbf{x},\boldsymbol{\xi},\theta)=z+\zeta-\mathrm{i}[(x-\xi)\cos\theta+(y-\eta)\sin\theta] \tag{6}$$

and the wavenumber integral function $K(Z,k_i)$ in (3) is expressed by

$$K(Z,k_i)=\mathrm{e}^{k_iZ}E_1(k_iZ)+\mathrm{i}\pi\big[\mathrm{sgn}(\mu_i)+\mathrm{sgn}(\mu_i\mathrm{v}-\kappa_i\mathrm{w})\big]H(\kappa_i)\,\mathrm{e}^{k_iZ}\quad\text{for}\quad i=1,2,3 \tag{7}$$

in [3] with the exponential integral function $E_1(\cdot)$ defined by Eq.5.1.1 in [7], the usual sign function $\mathrm{sgn}(\cdot)$ and the Heaviside function $H(\cdot)$. The single Fourier polar integral (3) is often referred as the representation of Havelock's type of the Green function.

# 3 Super Green function and its gradient

The surface integration of the Green function over the source surface associated with a field point is called S2P integral while the further integration of S2P integral over the field surface called S2S integral. The two-fold integration (S2S) is necessary in the evaluation of influence coefficients of the boundary integral equation based on the Galerkin scheme. First we consider a flat panel $S$ on which a constant source is applied. The panel is of polygonal form with $m$ vertices with the coordinates $Q_j(\xi_j,\eta_j,\zeta_j)$ for $j=1,2,\cdots,m$, and connectivities from $Q_j$ to $Q_{j+1}$ with $Q_{m+1}=Q_1$ to close the contour. The field point is denoted by $P(x,y,z)$ and the variable $Z_j(P,Q_j,\theta)$ connects $P(x,y,z)$ to $Q_j(\xi_j,\eta_j,\zeta_j)$ by its definition (6). Using the following notations

$$F(Z,\theta)=\sum_{i=1}^{3}A_iK(Z,k_i)\quad\text{and}\quad F_n(Z,\theta)=\sum_{i=1}^{3}A_iK_n(Z,k_i) \tag{8}$$

for $n\geq 1$, the integration of the Green function defined by (3) is then obtained by

$$\mathcal{G}^F(\mathbf{x})=\iint_S G^F(\mathbf{x},\boldsymbol{\xi})\,\mathrm{d}s(\boldsymbol{\xi})=\frac{1}{\pi}\int_{-\pi}^{\pi}\sum_{j=1}^{m}\big[c_jF_2(Z_j,\theta)+d_jF_1(Z_j,\theta)\big]\,\mathrm{d}\theta \tag{9}$$

developed in [8]. The geometry-dependent coefficients $(c_j,d_j)$ are defined by

$$\begin{aligned}
c_j&=(n_2+\mathrm{i}n_3\sin\theta)\big[(\xi_j-\xi_{j-1})\delta_{j-1}^c-(\xi_{j+1}-\xi_j)\delta_j^c\big]-(n_1+\mathrm{i}n_3\cos\theta)\big[(\eta_j-\eta_{j-1})\delta_{j-1}^c-(\eta_{j+1}-\eta_j)\delta_j^c\big]\\
d_j&=(n_2+\mathrm{i}n_3\sin\theta)\big[(\xi_j-\xi_{j-1})\delta_{j-1}^d+(\xi_{j+1}-\xi_j)\delta_j^d\big]-(n_1+\mathrm{i}n_3\cos\theta)\big[(\eta_j-\eta_{j-1})\delta_{j-1}^d+(\eta_{j+1}-\eta_j)\delta_j^d\big]
\end{aligned} \tag{10}$$

in which $\vec{n}=(n_1,n_2,n_3)$ is the normal vector of the surface $S$, and $(\delta_j^c,\delta_j^d)$ given by

$$\delta_j^c=\begin{cases}1/\Delta_j & \text{for}\quad|\Delta_j|>\epsilon_s\\ 0 & \text{for}\quad|\Delta_j|\leq\epsilon_s\end{cases}\qquad\text{and}\qquad\delta_j^d=\begin{cases}0 & \text{for}\quad|\Delta_j|>\epsilon_s\\ 1/2 & \text{for}\quad|\Delta_j|\leq\epsilon_s\end{cases} \tag{11}$$

with $\Delta_j=(\zeta_{j+1}-\zeta_j)+\mathrm{i}[(\xi_{j+1}-\xi_j)\cos\theta+(\eta_{j+1}-\eta_j)\sin\theta]$ for $j=1,2,\cdots,m$ and a tolerance $\epsilon_s=0.001$. It is worth noting that the subscript sequences $(\cdot)_0=(\cdot)_m$ and $(\cdot)_{m+1}=(\cdot)_1$ are to be taken in applying (10) to obtain $(c_j,d_j)$ and $\Delta_j$. In the same way, the integration of the derivatives of the Green function can be obtained and written as

$$\nabla\mathcal{G}^F(\mathbf{x})=\iint_S\begin{pmatrix}\partial_\xi\\ \partial_\eta\\ \partial_\zeta\end{pmatrix}G^F(\mathbf{x},\boldsymbol{\xi})\,\mathrm{d}s(\boldsymbol{\xi})=\frac{1}{\pi}\int_{-\pi}^{\pi}\begin{pmatrix}\mathrm{i}\cos\theta\\ \mathrm{i}\sin\theta\\ 1\end{pmatrix}\sum_{j=1}^{m}\big[c_jF_1(Z_j,\theta)+d_jF(Z_j,\theta)\big]\,\mathrm{d}\theta \tag{12}$$

involving the functions $(F_1,F)$ in place of $(F_2,F_1)$ in (9) with $(F_2,F_1,F)$ defined in (8). In the definition (8) of $F(Z,\theta)$ and $F_n(Z,\theta)$, the functions $K_n(Z,k_i)$ for $n\geq 1$ are successive antiderivatives of $K(Z,k_i)$, i.e.

$$\partial K_n(Z,k_i)/\partial Z=K_{n-1}(Z,k_i)\quad\text{for}\quad n\geq 1\quad\text{with}\quad K_0(Z,k_i)=K(Z,k_i) \tag{13}$$

with respect to $Z$. The work in [3] gives three expressions of antiderivatives:

$$K_n(Z,k_i) = k_i^{-n}\left[K(Z,k_i) + \sum_{m=0}^{n-1}(k_iZ)^m L_m(Z)\right] \tag{14}$$

$$\tilde{K}_n(Z,k_i) = \sum_{m=0}^{\infty}\left[K(Z_0,k_i) + \sum_{p=1}^{m}(-1)^p\frac{(p-1)!}{(k_iZ_0)^p}\right]\frac{(k_i\tilde{Z})^m}{(m+n)!}\tilde{Z}^n \tag{15}$$

$$\hat{K}_n(Z,k_i) = -\sum_{m=0}^{\infty}(k_iZ)^m Z^n \mathcal{L}_{m+n}(Z,k_i) \tag{16}$$

with

$$L_0(Z) = \ln(-Z) \quad \text{and} \quad L_m(Z) = [L_{m-1}(Z) - 1/m!]/m \quad \text{for} \quad m \geq 1 \tag{17}$$

used in (14) and

$$\mathcal{L}_0(Z,k_i) = \gamma + \ln(-k_i) + \ln(-Z) \quad \text{and} \quad \mathcal{L}_m(Z,k_i) = [\mathcal{L}_{m-1}(Z,k_i) - 1/m!]/m \quad \text{for} \quad m \geq 1 \tag{18}$$

in which $\gamma = 0.5772156649\ldots$ is the Euler's constant, $Z_0 = z_0 + \zeta_0 - \mathrm{i}[(x_0-\xi_0)\cos\theta + (y_0-\eta_0)\sin\theta]$ associated with a pair of reference points $(\mathbf{x}_0, \boldsymbol{\xi}_0)$, and $\tilde{Z} = Z - Z_0$, used in (15). All three antiderivatives $K_n$ by (14), $\tilde{K}_n$ by (15) and $\hat{K}_n$ by (16) are equivalent and have a different constant (indepedent of $Z$) between them which does not induce any difference in their applications to super Green functions.

Now we consider the field point $P(x,y,z)$ located within a flat panel $H$ of polygonal form with $\bar{m}$ vertices $P_\ell(x_\ell, y_\ell, z_\ell)$ for $\ell = 1, 2, \cdots, \overline{m}$. The side segments are denoted by the connection from $P_\ell$ to $P_{\ell+1}$ with $P_{\overline{m}+1} = P_1$ to close the contour. The second-fold integration of $\mathcal{G}^F(\mathbf{x})$ by (9) on the field panel $H$ is obtained by

$$\mathcal{G}^F = \iint_H \mathcal{G}^F(\mathbf{x})\,\mathrm{d}s(\mathbf{x}) = \frac{1}{\pi}\int_{-\pi}^{\pi}\sum_{j=1}^{m}\sum_{\ell=1}^{\overline{m}}\Big[c_j\bar{c}_\ell F_4(Z_{j\ell},\theta) + (c_j\bar{d}_\ell + d_j\bar{c}_\ell)F_3(Z_{j\ell},\theta) + d_j\bar{d}_\ell F_2(Z_{j\ell},\theta)\Big]\mathrm{d}\theta \tag{19}$$

in which the coefficients $(c_j, d_j)$ are given by (10) and $(\bar{c}_\ell, \bar{d}_\ell)$ by

$$\begin{aligned}
\bar{c}_\ell &= (\bar{n}_2 - \mathrm{i}\bar{n}_3\sin\theta)\big[(x_\ell - x_{\ell-1})\bar{\delta}^c_{\ell-1} - (x_{\ell+1} - x_\ell)\bar{\delta}^c_\ell\big] - (\bar{n}_1 - \mathrm{i}\bar{n}_3\cos\theta)\big[(y_\ell - y_{\ell-1})\bar{\delta}^c_{\ell-1} - (y_{\ell+1} - y_\ell)\bar{\delta}^c_\ell\big] \\
\bar{d}_\ell &= (\bar{n}_2 - \mathrm{i}\bar{n}_3\sin\theta)\big[(x_\ell - x_{\ell-1})\bar{\delta}^d_{\ell-1} + (x_{\ell+1} - x_\ell)\bar{\delta}^d_\ell\big] - (\bar{n}_1 - \mathrm{i}\bar{n}_3\cos\theta)\big[(y_\ell - y_{\ell-1})\bar{\delta}^d_{\ell-1} + (y_{\ell+1} - y_\ell)\bar{\delta}^d_\ell\big]
\end{aligned} \tag{20}$$

involving the normal vector $\vec{n} = (\bar{n}_1, \bar{n}_2, \bar{n}_3)$ on the panel $H$ and $(\bar{\delta}^c_\ell, \bar{\delta}^d_\ell)$ given by

$$\bar{\delta}^c_\ell = \begin{cases} 1/\bar{\Delta}_\ell & \text{for} \quad |\bar{\Delta}_\ell| > \epsilon_s \\ 0 & \text{for} \quad |\bar{\Delta}_\ell| \leq \epsilon_s \end{cases} \qquad \text{and} \qquad \bar{\delta}^d_\ell = \begin{cases} 0 & \text{for} \quad |\bar{\Delta}_\ell| > \epsilon_s \\ 1/2 & \text{for} \quad |\bar{\Delta}_\ell| \leq \epsilon_s \end{cases} \tag{21}$$

with $\bar{\Delta}_\ell = (z_{\ell+1} - z_\ell) - \mathrm{i}[(x_{\ell+1} - x_\ell)\cos\theta + (y_{\ell+1} - y_\ell)\sin\theta]$ for $\ell = 1, 2, \cdots, \overline{m}$. Again, the subscript sequences $(\cdot)_0 = (\cdot)_{\overline{m}}$ and $(\cdot)_{\overline{m}+1} = (\cdot)_1$ are implied in the application of (20) to obtain $(\bar{c}_\ell, \bar{d}_\ell)$ and $\bar{\Delta}_\ell$. Furthermore, The variables $Z_{j\ell}$ is defined by $Z_{j\ell} = z_\ell + \zeta_j - \mathrm{i}[(x_\ell - \xi_j)\cos\theta + (y_\ell - \eta_j)\sin\theta]$. In the same way, the integration of $\nabla\mathcal{G}^F(\mathbf{x})$ on the field panel $H$ is expressed by

$$\nabla\mathcal{G}^F = \iint_H \nabla\mathcal{G}^F(\mathbf{x})\,\mathrm{d}s(\mathbf{x}) = \frac{1}{\pi}\int_{-\pi}^{\pi}\begin{pmatrix}\mathrm{i}\cos\theta \\ \mathrm{i}\sin\theta \\ 1\end{pmatrix}\sum_{j=1}^{m}\sum_{\ell=1}^{\overline{m}}\Big[c_j\bar{c}_\ell F_3(Z_{j\ell},\theta) + (c_j\bar{d}_\ell + d_j\bar{c}_\ell)F_2(Z_{j\ell},\theta) + d_j\bar{d}_\ell F_1(Z_{j\ell},\theta)\Big]\mathrm{d}\theta \tag{22}$$

involving the functions $(F_3, F_2, F_1)$ in place of $(F_4, F_3, F_2)$ in (19) with $F_n$ for $n \geq 1$ defined in (8) using the antiderivatives $K_n(Z,k_i)$ given by (14)–(16) of the wavenumber integral function $K(Z,k_i)$ defined by (7).

# 4 Numerical results and discussions

The ship-motion Green function is expressed as a double Fourier integral and its surface integration on the source panel results in a four-fold integration or six-fold integration if the second surface integral on the field panel is performed according to the Galerkin scheme. The four-fold (or six-fold) integration is reduced to a single integral of Fourier polar angle, thanks to Havelock's representation of the Green function by analytical integration with Fourier wavenumber as the inner integral, and analytical surface integration on flat panels summarized in the aforegoing.

The surface integration of the wavenumber integral function $K(Z,k_i)$ involves its antiderivatives $K_n(Z,k_i)$ with respect to $Z$, and geometrical coefficients $(c_j, d_j)$ and $(\bar{c}_\ell, \bar{d}_\ell)$ of flat panels. There are three equivalent expressions (14)–(16) which are complementary in numerical applications. The original expression (14) denoted by $K_n(Z,k_i)$ is well suited for computations when $F_r^2 k_i$ is of order $O(1)$ or larger, which is the case for $k_2$ and $k_3$, also for $k_1$ when

Table 1: Coordinates of panels' vertices scaled with the reference length $L = 1m$

| No | $H(x, y, z)$ | $S_1(x, y, z)$ | $S_2(x, y, z)$ |
|---|---|---|---|
| 1 | (-0.681511, -0.239974, -0.033530) | (-1.407723, -0.504959, 0.0) | (2.111993, -1.626152, 0.0) |
| 2 | (-0.681511, -0.245641, -0.017905) | (-1.539255, -0.665065, 0.0) | (2.027278, -1.449003, 0.0) |
| 3 | (-0.748460, -0.234381, -0.017905) | (-1.605234, -0.622041, 0.0) | (2.102859, -1.428670, 0.0) |
| 4 | (-0.748460, -0.228974, -0.033530) | (-1.468064, -0.472292, 0.0) | (2.193806, -1.597798, 0.0) |

$F_r^2 k_1 \approx O(1)$. For small $\omega$ and $F_r^2 k_1 \approx \tau^2$, the formulations (15) denoted by $\tilde{K}_n(Z, k_1)$ and (16) by $\hat{K}_n(Z, k_1)$ are preferred. Among $\tilde{K}_n(Z, k_1)$ and $\hat{K}_n(Z, k_1)$, it is preferred to use (15) when the reference distance $Z_0$ between two panels is large.

Super Green function (S2S integral) is evaluated with three typical panels: one $H$ on Wigley hull and two $(S_1, S_2)$ on the mean free surface. The coordinates of 4 vertices of panels are listed in Tab.1. The first test concerns the two panels $S_1$ and $S_2$, and surface integration of $K(Z, k_1)$ is carried out by using antiderivatives (14)–(16) for $\omega = 0.9$ and $\tau = 0.27$ with $\epsilon = 0.001$. The results by using (14) in which the numerical accuracy of $K(Z, k_1)$ is limited to 6 digits, presented on the left of Fig.1, are not good since very small $F_r^2 k_1 = 0.0729$ while those by using (15) are globally good except in the vicinity of $\theta/\pi = -0.58$ and $\theta/\pi = 0.42$ where $k_1 Z_0 < 2$. On the other side, the results using (16) are accurate in these intervals where $k_1 Z_0$ is small. In general, the numerical accuracy of formulation (14) is good for $F_r^2 k_1 > 0.4$ while the formulation (16) is efficient for $k_1 Z_0 < 10$ and that (15) for $k_1 Z_0 > 6$. The second test case concerns the panels $H$ and $S_1$ for $\omega = 3$ and $\tau = 0.9$ with $\epsilon = 0.001$. Numerical results by the Gauss-Legendre quadrature, presented on the right of Fig.1, are carried out with $1\times1$, $2\times2$ and $8\times8$ Gauss points on the panels and compared with those by analytical integration (19) in which the integrand function is augmented by summing the part for $\theta \in [-\pi, 0]$. The values of SGF presented in Fig.1 are scaled with $F_r^6$. It is shown that the analytical integration using (14)-(16) in a complementary way is accurate and efficient.

# References


[1] F. Noblesse, X.B. Chen & C. Yang (1999) Generic Super Green functions. *Ship Technology Research*, (46).

[2] J.V. Wehausen & E.V. Laitone (1960) Surface waves. *Handbuch der Physik*.

[3] X.B. Chen (2023) Fundamental solutions to ship-motion problems with viscous effects. *Physics of Fluids* (35).

[4] F. Ursell (1960) On Kelvin's ship-wave pattern. *J. Fluid Mech.*, (8), pp418–431.

[5] X.B. Chen & G.X. Wu (2001) On singular and highly oscillatory properties of the Green function for ship motions. *J. Fluid Mech.*, (445), pp77–91.

[6] X.B. Chen, M.Q. Nguyen, I. Ten, C. Ouled Housseine, Y.M. Choi, L. Diebold, S. Malenica, G. De-Hautecloque & Q. Derbanne (2022) New seakeeping computations based on potentials linearised over the ship-shaped stream. *Proc. 15th Intl PRADS'2022, Dubrovnik, Croatia.*

[7] M. Abramowitz & I.A. Stegun (1972) Handbook of Mathematical Functions with Formulas, Graphs, and Mathematical Tables *National Bureau of Standards.*

[8] X.B. Chen, Y.M. Choi & M.Q. Nguyen (2025) Super Green functions associated with a source distribution on ship hull and over free surface. *In prepration.*


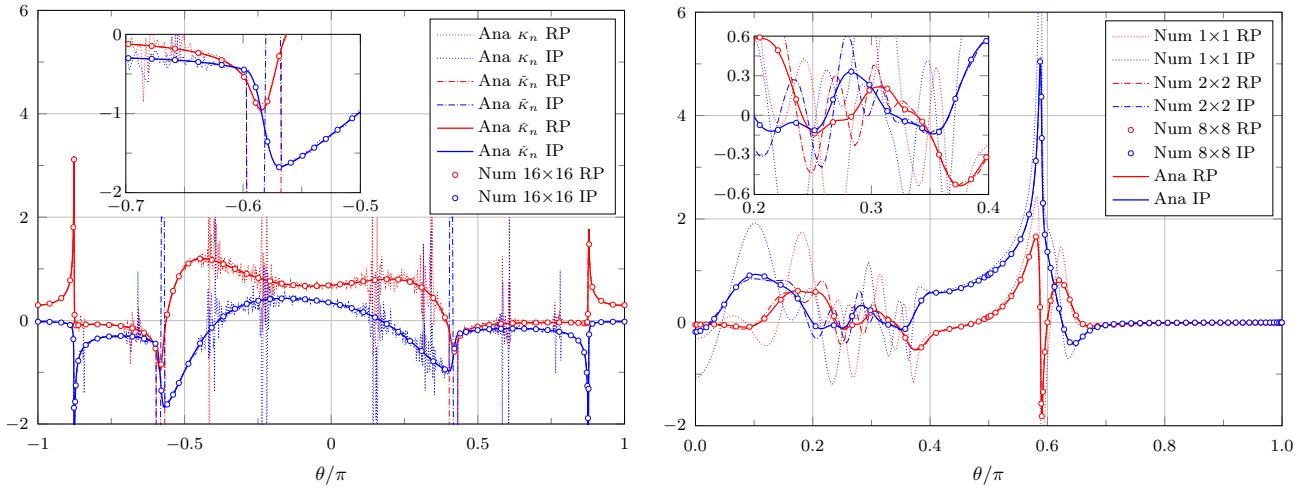


Figure 1: Comparison of numerical integration and analytical integration